The study of $Al_{0.29}Ga_{0.71}N$ and AlN cap layers grown on GaN/AlN/Si(111) by RF plasma assisted MBE

M. Z. MOHD YUSOFF[a,b], A. MAHYUDDIN[b], A. BAHARIN[b], Z. HASSAN[b], H. ABU HASSAN[b], M. J. ABDULLAH[b]
[a]*Department of Applied Sciences, Universiti Teknologi MARA (UiTM), 13500 Permatang Pauh, Penang, Malaysia*
[b]*Nano-Optoelectronics Research and Technology Laboratory, School of Physics, Universiti Sains Malaysia, 11800 Penang, Malaysia*

In this work, the growth and characterization of epitaxial $Al_{0.29}Ga_{0.71}N$ and AlN cap layers grown on GaN/AlN/Si(111) substrate by RF-plasma assisted molecular beam epitaxy (MBE) are described. The Al mole fraction of x=0.29 was derived from the HR-XRD symmetric rocking curve (RC) ω/2θ scans of (0002) plane. For AlN/GaN/AlN sample, the maximum Raman intensity at 521.53 cm^{-1} is attributed to crystalline silicon. The allowed Raman optical phonon mode of GaN, E_1 (high) located at 570.74 cm^{-1} is clearly visible. PL spectrums of both samples have shown sharp and intense band edge emission of GaN without the existence of yellow emission band, indicating that good crystal quality of the samples have been successfully grown on the Si substrate. For IR reflectance analysis, GaN-like and AlN-like E_2 (TO) optical modes have been measured at 558 cm^{-1} and 667 cm^{-1} respectively for $Al_{0.29}Ga_{0.71}N$ cap layer. Finally, *I-V* measurement has been conducted to verify the rectifying characteristic of both samples.

(Received April 4, 2012; accepted October 30, 2012)

Keywords: III-Nitrides, GaN, AlN, MBE, Silicon substrate

1. Introduction

$Al_xGa_{1-x}N$ alloys are extremely important materials with widespread applications for optoelectronic devices because they have a direct wide energy bandgap, which ranges from 3.4 to 6.2 eV. Due to their wide band gap range, these alloys are very attractive materials for applications in ultraviolet (UV) laser diodes (LDs), light emitting diodes (LEDs) and photodetectors [1-3]. AlN, which has the widest direct band gap (~6.1 eV) among the III-nitrides and possesses outstanding properties such as high temperature stability, high thermal conductivity, and deep ultraviolet (DUV) transparency [4]. Furthermore, AlN thin films are potentially excellent insulators due to a high dielectric constant ε of 9.14 [5], good thermal conductivity of 2.85 W/cmK, and have a breakdown electric field higher than 3.3 MV/cm [6].

Silicon substrate presents the obvious advantages since it is a well-established technology, low cost and has the potential for hybrid integration. However, Si (111) has been less investigated than sapphire as a substrate to grow nitrides, due to the higher lattice and thermal expansion coefficient mismatches resulting in a higher dislocation density and the potential generation of crack [7]. In addition, the problems of interdiffusion at the Si/epilayer interfaces increases the difficulty of interpretation the electrical measurements [8].

In this paper, we report on the growth of two III-nitrides thin films samples on Si(111) substrates with different growth condition, using high-temperature-grown GaN/AlN as a buffer layer. The growth was performed using plasma assisted molecular beam epitaxy (PA-MBE). The structural and optical studies of the samples were investigated using high resolution X-ray diffraction (HR-XRD), Raman spectroscopy and photoluminescence (PL) spectroscopy. Fourier transforms infrared (FTIR) spectrometer (Spectrum GX FT-IR, Perkin-Elmer) was also used to perform the IR reflectance measurement. To verify the rectifying characteristic of both samples; the current-voltage (*I-V*) measurement was conducted.

2. Experimental works

All samples were grown in Veeco Gen II MBE system, with radio-frequency plasma source. The 3-inch Si (111) substrate was ex-situ cleaned with standard cleaning procedure by using RCA method prior entry into the MBE system. The substrates were outgassed at 900 ^oC for 2 hours in ultra-high vacuum. In order to remove SiO_2 from the surface of silicon, a few monolayers of Ga were deposited on the substrate to form Ga_2O_3. A clean Si (111) can be observed from the presence of prominent Kikuchi lines in the typical Si (111) 7 x 7 surface reconstruction pattern. To prevent formation of Si_3N_4 at the surface, a few monolayers of Al were deposited before the nitrogen source was activated.

$Al_xGa_{1-x}N$ @ 861^{0}C @ 0.225µm
GaN @ 840^{0}C @ 0.081µm
AlN @ 875^{0}C @ 0.031µm
Si (111)

(a)

AlN @ 850^{0}C @ 0.208µm
GaN @ 870^{0}C @ 0.414µm
AlN @ 870^{0}C @ 0.149µm
Si (111)

(b)

Fig.1. Cross-section structures of (a) $Al_xGa_{1-x}N$ and (b) AlN cap layers on GaN/AlN/Si sample.

For $Al_xGa_{1-x}N$ cap layer on GaN/AlN/Si (111) sample, AlN buffer layer was initially grown on the Si substrate for 13 minutes with the substrate temperature set at 875°C. Subsequently, GaN epilayer was grown on top of the buffer layer for 20 minutes with the substrate temperature set at 840°C. To grow $Al_xGa_{1-x}N$, the effusion cells of Al, and Ga were heated up to 1005 and 923°C, respectively. During the growth of $Al_xGa_{1-x}N$, the substrate temperature was set at 861°C (see Figure 1(a)). Similarly, for AlN cap layer on GaN/AlN/Si (111) sample, the buffer or wetting layer, AlN was initially grown on the Si substrate. To grow AlN buffer layer, the substrate temperature was heated up to 870^{o}C, in which both of the Al and N shutters were opened simultaneously for 15 minutes. Subsequently, GaN epilayer was grown on top of the AlN layer for 60 minutes. The temperature for the growth of GaN in the AlN/GaN/AlN is 870^o C. Finally, AlN thin layer was grown on GaN/AlN/Si(111) for 5 minutes with the substrate temperature set at 850^{o}C (see Figure 1(b)).

The MBE grown $Al_xGa_{1-x}N$ and AlN cap layers on GaN/AlN/Si(111) sample were characterized by a HR-XRD, Raman spectroscopy and PL system. HR-XRD with a Cu-Kα1 radiation source (λ= 1.5406Å) was used to assess and determine the crystalline quality of the epilayers. For PL system, a He-Cd laser with emission wavelength of 325 nm is used as the excitation source, in order to study the band gap and quality of these alloys. Fourier transforms infrared (FTIR) spectrometer (Spectrum GX FT-IR, Perkin-Elmer) with a potassium bromide (kBr) beam splitter and a mid IR triglycine sulface (TGS) detector are used to perform the IR reflectance measurement.

3. Results and discussions

The growth mode of the AlGaN cap layers was analysed using RHEED. Figure 2 shows the schematic of the evolution the AlGaN layer with the corresponding RHEED patterns. The Si substrate surface showed a clear surface reconstruction at high temperature as shown in Fig. 2(a). Starting from a smooth AlN buffer layer [Fig. 2(b)], the RHEED image remains streaky during initial stage of GaN growth. After the growth of GaN, the RHEED image continue to display a streaky pattern indicative of good surface morphology as revealed in Fig. 2(c). During the growth of GaN (Fig. 2(c)), the streaky RHEED pattern is sharpened, suggesting the improvement of the crystalline quality of GaN relative to the AlN buffer layer. In Fig. 2(d) $Al_xGa_{1-x}N$ growth under low temperature condition follows a Stranski-Krastanow growth mode, leading to $Al_xGa_{1-x}N$ on top of a continuous wetting layer.

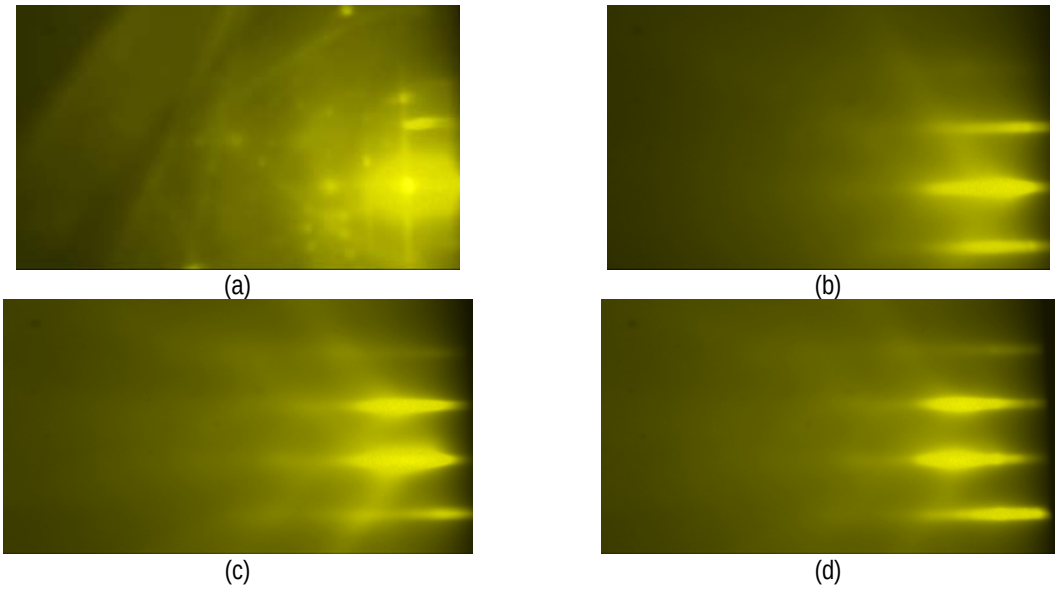

Fig. 2. RHEED pattern for the growth process of AlGaN cap layer on GaN/AlN/Si(111)

Fig. 3 showed that the sample with $Al_xGa_{1-x}N$ cap layer has also been successfully grown on GaN/AlNsilicon substrate and as confirmed from the presence of the peaks at 34.575°, 35.025° and 36.075°, which correspond to GaN (0002), $Al_xGa_{1-x}N$ (0002) and AlN (0002), respectively. XRD symmetric RC ω/2θ scans of (0002) plane at room temperature was also conducted to verify the crystalline quality of thin films. The full width at half-maximum (FWHM) of $Al_xGa_{1-x}N$ was 0.528°, which can be seen from Fig. 4.

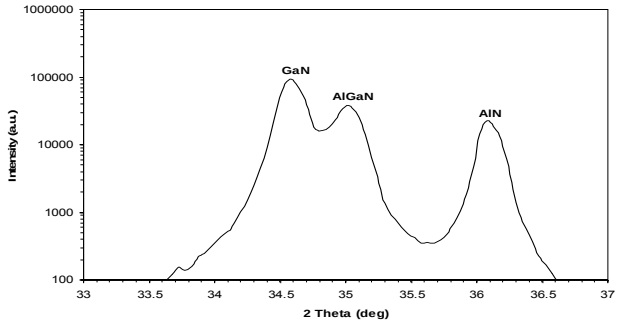

Fig. 3. XRD spectrum of the $Al_xGa_{1-x}N$ cap layer taken from the (0002) diffraction plane.

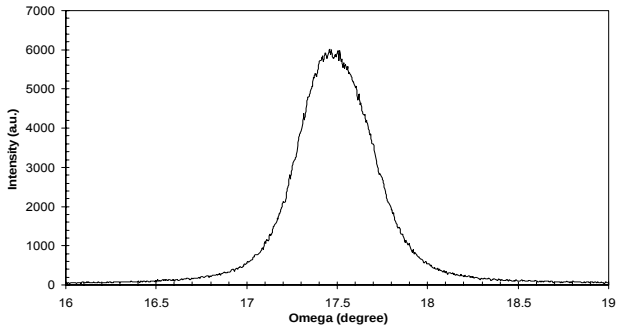

Fig. 4. XRD symmetric RC ω/2θ scans of (0002) plane for $Al_xGa_{1-x}N$ cap layer grown on GaN /GaN/AlN/Si sample.

From the XRD symmetric RC ω/2θ scans of (0002) plane, the lattice parameter c of the samples can be calculated using the following formula:

$$c = \frac{\lambda l}{2\sin\theta_{RC}} \tag{1}$$

where λ is the wavelength of the x-ray radiation (1.5406 Å), θ_{RC} is the Bragg angle estimated from the peak of the RC, and □ is the Miller indices. In principle, the composition can be determined through XRD measurements and application of Vegard's law. By assuming the layers are fully relaxed or fully strained, according to Vegard's law, the variation of the lattice constant c between GaN and AlN is linearly proportional to the Al mole fraction [9]. Based on the obtained c value, the mole composition of the Al, x, can be determined using the following formula [10]:

$$x = \frac{\left(c_{AlGaN} - c_{GaN}\right)}{\left(c_{AlN} - c_{GaN}\right)} \tag{2}$$

where c_{GaN}, c_{AlN} and c_{AlGaN} are the lattice constants of GaN, AlN, and $Al_xGa_{1-x}N$, respectively. From equations (1) and (2), the mole fraction x of $Al_xGa_{1-x}N$ can be calculated. According to this law and equation (1) and (2), Al mole-fraction was determined as 0.29 for $Al_{0.29}Ga_{0.71}N$ sample.

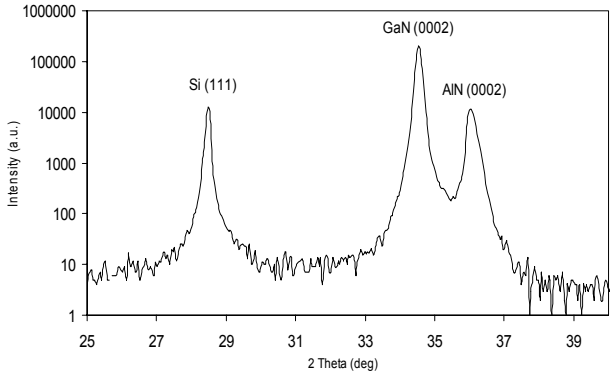

Fig. 5. XRD spectra of the AlN cap layer taken from the (0002) diffraction plane and measured by the 2 Theta – Omega scan mode.

Fig. 5 showed that AlN cap layer on GaN/AlN/Si sample has also been successfully grown on silicon substrate and has been confirmed from the presence of the peaks at 28.475°, 35.525° and 36.075^0, which correspond to Si (111), GaN (0002) and AlN (0002), respectively.

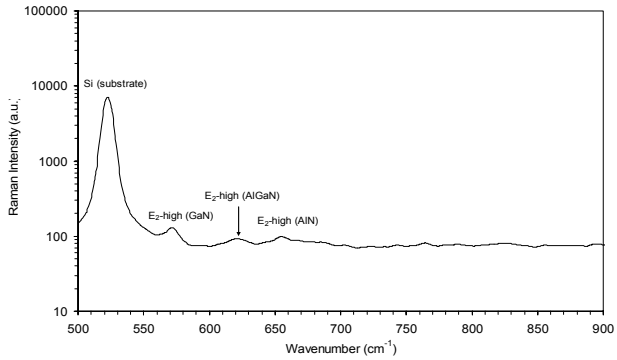

Fig. 6. Room temperature Raman spectrum of $Al_{0.29}Ga_{0.71}N$ cap layer on GaN/AlN/Si(111) substrate

In order to understand the role of the buffer layers, micro-Raman scattering is used to investigate the stress status of the as-grown samples in further detail. Fig. 6 shows the Raman spectrum of as-grown $Al_{0.29}Ga_{0.71}N$ cap layer on GaN/AlN/Si sample. The dominant E_2 (high)

phonon mode of GaN appears at 572.7 cm^{-1}. The E_2 (high) mode of AlN appears at 656.7 cm^{-1} and deviates from the standard value of 655 cm^{-1} for unstrained AlN [11]. Finally, the weak phonon mode at 622.5 cm^{-1} is attributed to the $Al_{0.29}Ga_{0.71}N$ E_2 (high) phonon mode [12-14]. The E_2 (high) modes in the Raman spectra can be used to estimate the stress because it has been proven to be particularly sensitive to biaxial stress present within the samples [15]. The broadening in alloy semiconductors has been attributed to defects and/or inhomogeneous stress and/or the inhomogeneous distribution of constituent atoms [15]. It has been known that the line width E_2(H) reflects the crystalline quality [16] and can be an indicator of the degree of randomness of the alloy [17].

Figure 7 shows the Raman spectrum for the AlN cap layer on GaN/AlN/Si(111). The maximum intensity at 521.53 cm^{-1} is attributed to crystalline silicon. It was found that the allowed Raman optical phonon mode of GaN, the E_1 (high)) is clearly visible, which is located at 570.74 cm^{-1}. The presence of E_1 (high) has led to the evidence of hexagonal-phase character for this GaN buffer layer. The use of silicon (111) substrate for growth of III-nitrides, particularly GaN, always produces relatively low crystal quality; therefore it is difficult to grow high quality GaN-based materials on silicon (111) substrate [18-20]. It has been proposed that the large difference in lattice constant, crystal structure and thermal expansion coefficient between the silicon and GaN-based materials are amongst several factors which contributed to the poor crystal quality of the GaN-based epilayers [21].

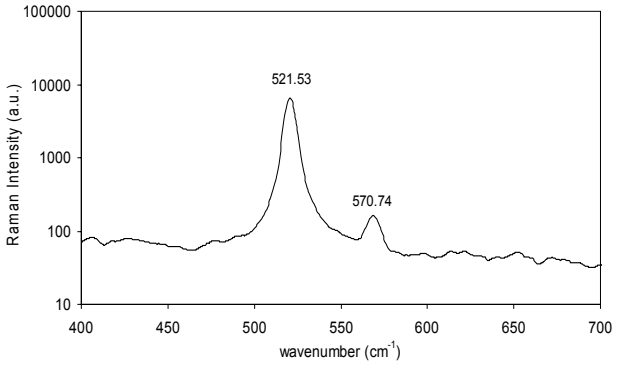

Fig. 7. Room temperature Raman spectrum of AlN cap layer on GaN/AlN/Si (111)

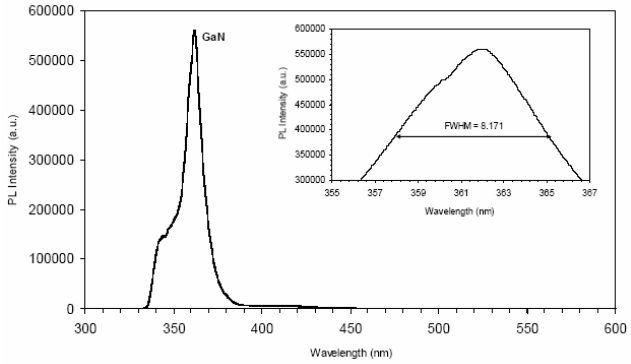

Fig. 8. PL spectra of the $Al_{0.29}Ga_{0.71}N$ cap layer on GaN/AlN/Si sample

Fig. 8 and 9 shows the PL spectrum of the $Al_{0.29}Ga_{0.71}N$ and AlN cap layers, respectively. The PL spectrums for the $Al_{0.29}Ga_{0.71}N$ and AlN cap layers are dominated by the intense and sharp peaks at 362.31 nm and 363.23 nm respectively, which are attributed to the band edge emission of GaN. The band edge emission for $Al_{0.29}Ga_{0.71}N$ cap layer was not obtained due to the limitation of the excitation source used in this study. No yellow band emissions were observed either; this indicates that the thin films are of good optical quality. For AlN cap layer sample, the peak at 387.22 nm is probably due to impurities or native defects (such as C or N vacancy, Ga vacancy) related recombination. There is another broad peak located at 727.46 nm; the presence of this broad peak is rarely observed in n-type GaN PL studies (see Figure 9 (inset)). This peak can be as attributed to red luminescence which has been reported by many researchers [22-26]. The origin of this peak could be the result of transition between a $N_{Ga\ site} - Ga_{N\ site}$ deep donor-deep acceptor state [27].

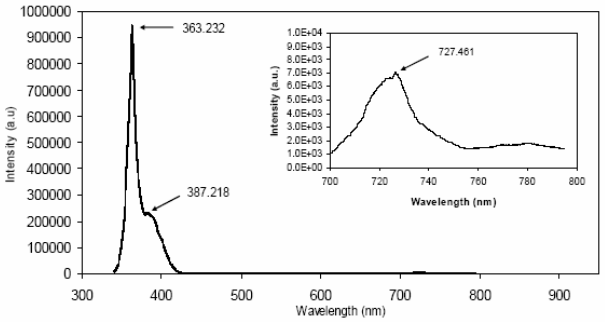

Fig. 9. PL spectra of the AlN cap layer on GaN/AlN/Si(111) sample.

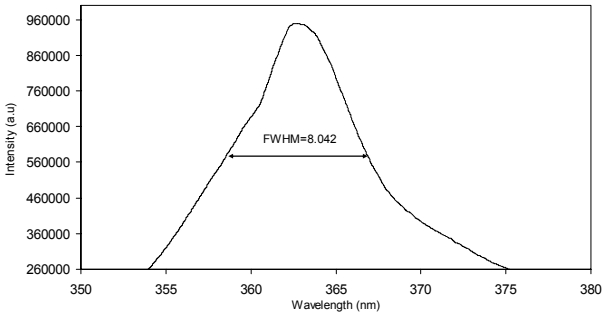

Fig. 10. FWHM measured for PL spectra of the AlN cap layer on GaN/AlN/Si(111) sample.

In the literature, the PL peak width obtain from the PL spectra is often used to characterize the quality of the material. Therefore, for GaN peak in $Al_{0.29}Ga_{0.71}N$/GaN/AlN/Si(111) sample, the full width at half-maximum (FWHM) is 8.171 nm, as shown in Figure 8 (inset). Meanwhile, for GaN peak in AlN/GaN/AlN/Si(111) sample, the FWHM is 8.042 nm (see Figure 10). Both FWHM of samples are quiet comparable to that observed from the literature reviews [28, 29]. In general, the sample with smaller FWHM of the

PL peak will have a better optical quality, for which there is a smaller band gap fluctuation amplitude [30-31].

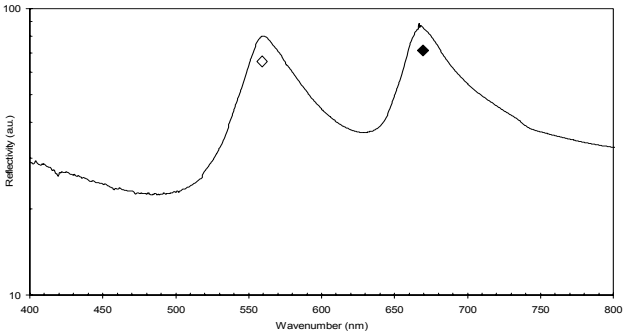

Fig. 11. IR reflectance spectra of the $Al_{0.29}Ga_{0.71}N$ cap layer on GaN/AlN/Si sample.

Under IR reflectance measurement, purely transverse optical (TO) and longitudinal optical (LO) phonon modes can be observed for phonon propagation direction perpendicular and parallel to the crystal axis; hence, more strongly marked features can be obtained [32]. Fig. 11 shows the IR reflectance spectra of the $Al_{0.29}Ga_{0.71}N$ cap layer on GaN/AlN/Si(111) substrate. The GaN-like and AlN-like E_1(TO) optical modes of the $Al_{0.29}Ga_{0.71}N$ cap layer are represented by the open (◊) and close (♦) symbols, respectively. The large reflectivity features in the spectra have altered to form two peaks centered at ~558 cm^{-1} and 667 cm^{-1}, indicating that the incorporation of the Al elements into the semiconductor have created dramatic changes to the lattice dynamics of the material [27]. The broadening of the IR peaks for the GaN-like and AlN-like E_1 (TO) optical modes of the $Al_{0.29}Ga_{0.71}N$ cap layer may presumably represent the weakening of the bond strength in the films [33]. Hence, the structure of these films may be considered to be in polycrystalline or microcrystalline phase.

Figs. 12-13 shows the current voltage (I-V) characteristics of $Al_{0.29}Ga_{0.71}N$ and AlN cap layers grown on GaN/AlN/Si(111) substrate, operating under forward and reverse biases. Both samples shows the typical rectifying characteristics and the results are quiet comparable with Chuah et al. [34, 35]. It is well known that GaN contains high amount of defect densities especially due to reason like the difference in the thermal expansion coefficient and large lattice mismatch between GaN material and the substrate, particularly those grown on Si [36-39]. The high amount of current observed can be attributed to the tunneling of carrier across the barrier. This effect can be enhanced by the interfacial layer to produce trap-assisted tunnel currents. The existence of a thin interfacial layer can be ruled out unless the semiconductor is cleaved in an ultra-high vacuum condition [40, 41].

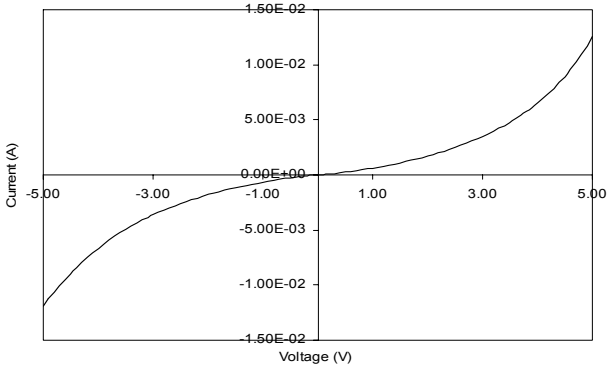

Fig. 12. IV Characteristic of $Al_{0.29}Ga_{0.71}N$ cap layer on GaN/AlN/Si(111) substrate

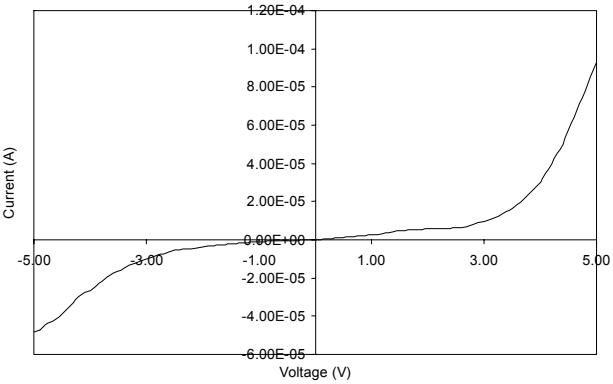

Fig. 13. IV Characteristic of AlN cap layer on GaN/AlN/Si(111) substrate

4. Conclusions

In summary, the growth of $Al_{0.29}Ga_{0.71}N$ and AlN cap layers on GaN/AlN/Si(111) substrate has been successfully performed using plasma-assisted molecular beam epitaxy. The microstructure and optical properties of the material has been revealed using XRD, Raman, FTIR and PL. The Al mole fraction was derived from the HR-XRD symmetric rocking curve (RC) ω/2θ scans of (0002) plane. For AlN/GaN/AlN sample, the maximum Raman intensity at 521.53 cm^{-1} is attributed to crystalline silicon. The allowed Raman optical phonon mode of GaN, the E_1 (high) is clearly visible, which is located at 570.74 cm^{-1}. PL spectrums of both samples have shown sharp and intense band edge emission of GaN without the existence of yellow emission band, indicating good crystal quality of the samples have been successfully grown on the Si substrate. For the AlN cap layer sample, the observed peak at 387.22 nm is most likely due to the presence impurities or native defects (such as C or N vacancy, Ga vacancy) related recombination. GaN-like and AlN-like E_2 (TO) optical modes have been detected at 558 cm^{-1} and 667 cm^{-1} respectively, for $Al_{0.29}Ga_{0.71}N$ cap layer. Finally, for *I-V* measurement for both samples have shown the good typical rectifying characteristics and the results are quiet comparable with those reported in the literature.

Acknowledgements

The support from Universiti Teknologi MARA (UiTM) for excellence fund (600-RMI/ST/DANA 5/3/Dst (129/2010) is gratefully acknowledged.

References

[1] J.C. Carrano, T. Li, D.L. Brown, P.A. Grudowski, C.J. Eiting, R.D. Dupuis, J.C. Campbell. Electron. Lett. **34**, 1779 (1998).
[2] K. Zhu, M.L. Nakarmi, K. H. Kim, Appl. Phys. Lett. **85**, 4669 (2004).
[3] F. Omne`s, N. Marenco, B. Beaumont, Ph. De Mierry, E. Monoroy, F. Calle and E. Munoz. J. Appl. Phys. **86**, 5286 (1999).
[4] B.N. Pantha, R. Dahal, M.L. Nakarmi, N. Nepal, J. Li, J.Y. Lin, H.X. Jiang, Q.S. Paduano, David Weyburne. Appl. Phys. Lett. **90**, 241101 (2007).
[5] A.T. Collins, E.C. Lightowlers, P.J. Dean. Phys. Rev. **158**, 833 (1967).
[6] D. Cho, M. Shimizu, T. Ide, H. Ookita, H. Okumura, Jpn. J. Appl. Phys. **41,**.4481 (2002).
[7] J.L. Pau, E. Monroy, E. Munoz, F.B. Naranjo, F. Calle, M.A. Sanchez-Garcia, E. Calleja. J. Crystal Growth **230**, 544 (2001).
[8] E. Calleja, M.A. Sanchez-Garcia, D. Basak, F. J. Sanchez, F. Calle, P. Youinou, E. Munoz, J. J. Serrano, J.M. Blanco, C. Villar, T. Laine, J. Oila, K. Saarinen, P. Hautojarvi, C.H. Molloy, D.J. Somerford, I. Harrison. Phys. Rev. B **58,** 1150 (1998).
[9] L. Vegard. Die Konstitution der Mischkristalle und die Raumfüllung der Atome Phys., **5**, 17 (1921).
[10] C. G. V. d. Walle, M. D. McCluskey, C. P. Master, L. T. Romano, N.M. Johnson. Mat. Sci. Eng. **B59,** 274 (1999).
[11] M. Prokofyena, J. Seon, M. Vanbuskirk, S.A. Holtz, N.N. Nikishin, H. Temkin, S. Zollner. Phys. Rev. B **63**, 125313 (2001).
[12] J. Gleize, M.A. Renucci, J. Frandon, E. Bellet-Amalric, B. Baudin, J. Appl. Phys. **93**, 2065 (2003).
[13] F. Demangeot, J. Groenen, J. Frandon, M.A. Renucci, O. Briot, S. Clur, R.L. Aulombard, Appl. Phys. Lett. **72**, 2674 (1998).
[14] D. Rudloff, T. Riemann, J. Christen, Q.K.K. Liu, A. Kaschner, A. Hoffmann, CH. Tomsen, K. Vogeler, M. Diesselberg, S. Einfeldt, D. Hommel. Appl. Phys. Lett. **82**, 367 (2003).
[15] N. H. Zhang, X. L. Wang, Y. P. Zeng, H. L. Xiao, J. X. Wang, H. X. Liu, J. M. Li, J. Crystal Growth **280**, 346 (2005).
[16] M. Kuball. Surf. Interface Anal., **31**, 987 (2001).
[17] L. Bergman, M.D. Bremser, W.G. Perry, R.F. Davis, M. Dutta, R.J. Nemanich, Appl. Phys. Lett., **71**, 2157 (1997).
[18] A. Ohtani, K. S. Stevens, R. Beresford. Appl. Phys. Lett. **65,** 61 (1994).
[19] W. Ju, D. A. Gulino, R. Higgins. J. Cryst. Growth **263**, 30 (2004).
[20] J. Ristic, M. A. Sanchez-Garcia, E. Calleja, A. Perez-Rodriguez, C. Serre, A., Morante, J. R. Romanop Rodriguez, V. R. Koegler, W. Skorupa. Mat. Sci. Eng. B **93**, 172 (2002).
[21] T. Lei, M. Fanciulli, R.J. Molna, T. D. Moustakas, R. J. Graham, J. Scanlon. Appl. Phys. Lett. **59**, 944 (1991).
[22] D.M. Hofmann, B.K. Meyer, H. Alves, F. Leither, W. Burkhard, N. Romanov, Y. Kim, J. Kruger, E.R. Weber. Phys. Stat.Sol. (a), **180**, 261 (2000).
[23] S. Nakamura, N. Iwasaki, M. Senoh, T. Mukai. Jpn. J. Appl. Phys., 31, Part 1: pp.1258-1266 (1992).
[24] W. Gotz, L.T. Romano, B.S. Krusor, N.M. Johnson R.J. Molnar. Appl. Phys. Lett. **69**, 242 (1996).
[25] U. Kaufmann, M. Kunzer, H. Obloh, M. Maier, Ch. Manz, A. Ramakrishnan and B. Santic. Phys. Rev. B, **59**, 5561 (1999).
[26] M.W. Bayerl, M.S. Brandt, E.R. Glaser, A.E. Wickenden, D.D. Koleske, R.L. Henry, M. Stutzmann. Phys. Stat. Sol. (b), **216,**.547 (1999).
[27] S.S. Ng. Structural and Optical Studies of Wide Band-Gap $Al_xGa_{1-x}N$ ($0 \leq x \leq 1$) Semiconductors. Phd Thesis, Universiti Sains Malaysia (2008).
[28] S.S. Ng, Z. Hassan, H. Abu Hassan, M.E. Kordesh. Mater. Sci. Forum, **517**, 69 (2006).
[29] Z. Hassan, S.S. Ng, G.L. Chew, F.K. Yam, M.J. Abdullah, M.R. Hashim and K. Ibrahim. Mater. Sci. Forum, **480-481**, 531 (2005).
[30] Y.H. Cho, T.J. Schmidt, S. Bidnyk, G.H., Song, J.J., Keller, S., Mishra, U.K., DenBaars, S.P. Phys. Rev. B, **61**, 7571 (2000).
[31] M. Smith, G.D. Chen, J.Y. Lin, H.X. Jiang, M.A. Khan, Q. Chen. Appl. Phys. Lett. **69**, 2837 (1996).
[32] T. Dumelow, T.J. Parker, S.R.P. Smith, D.R. Tilley. Surf. Sci. Rep., **17**, 151 (1993).
[33] J. Tauc. Amorphous and Liquid Semiconductors. London, Plenum Publishing Company Ltd (1974).
[34] L.S. Chuah, Z. Hassan, H. Abu Hassan, F.K. Yam, C.W. Chin, S.M. Thahab. International J. Modern Phys. B., **22**, 5167 (2008).
[35] L.S. Chuah, Z. Hassan, H. Abu Hassan, N.M. Ahmed. J. Alloys & Compounds., **481**, L15 (2009).
[36] S. Tomiya, K. Funato, T. Asatsuma, T. Hino, S. Kijima, T. Asano, M. Ikeda. Appl. Phys. Lett. **77**, 636 (2000).
[37] S.J. Pearton. GaN and Related Materials, Amsterdam: Gordon and Breach Science Publishers (1997).
[38] W. Gotz, N.M. Johnson, D.P. Bour, C. Chen, H. Liu, C. Kuo, W. Imler, Mater. Res. Soc. Symp. Proc. **395**, 443 (1996).
[39] P. Hacke, T. Detchprohm, K. Hiramatsu, N. Sawaki, K. Tadatomo, K. Miyake. J. Appl. Phys. **76**, 304 (1994).
[40] S. Averine, Y.C. Chan, Y.L. Lam. Appl. Phys. Lett. **77**, 274 (2000).
[41] E.H. Rhoderick, R.H. William. Metal Semiconductor Contacts, 2nd., New York: Oxford University Press (1988).

*Corresponding author: mzmy83@gmail.com